Mesopotamian journal of Computer Science
Vol. **(2024)**, 2024, **pp**. 34–43
DOI: https://doi.org/10.58496/MJCSC/2024/004; ISSN: 2958-6631
https://mesopotamian.press/journals/index.php/cs

Research Article

A Comparative study of Chest Radiographs and Detection of The Covid 19 Virus Using Machine Learning Algorithm

Shaimaa Q. Sabri[1], Jahwar Y. Arif[1], Ghada A. Taqa[2, *], Ahmet Çınar[3]

[1] *Department of Computer Sciences, College of Science, University of Zakho, Duhok, Iraq*
[2] *Department of Dental Basic Sciences, College of Dentistry, University of Mosul, Mosul, Iraq*
[3] *Department of Computer Engineering, College of Engineering, Fırat, University, Elazığ, Türkiye*

ARTICLE INFO

Article History
Received 29 Dec 2023
Revised: 05 Feb 2024
Accepted 19 Feb 2024
Published 11 Mar 2024

Keywords
Covid19
Decision Tree
K-Nearest Neighbors
Machine Learning
Support Vector Machine

ABSTRACT

The severe acute respiratory syndrome coronavirus 2 (SARS-CoV-2) outbreak that is causing coronavirus disease 2019 is being deemed a pandemic because of its quick spread around the globe. Because chest X-ray pictures have shown to be beneficial in monitoring a variety of lung disorders, they have recently been utilized to monitor COVID-19 disease. It takes time to manually analyze a lot of chest X-ray pictures. Several previous studies have suggested machine-learning (ML)-based techniques for COVID-19 detection from chest X-ray pictures as a solution to this issue. Though little effort has been made to use traditional machine learning (ML) methods, the majority of these investigations use deep learning (DL) based techniques. Conventional ML-based algorithms will be favored for implementation if they can yield identical outcomes as DL-based methods. In this effort, we constructed four classic ML-based models for COVID-19 identification, driven by the need to close the gap in the literature. The accuracy rates for the various classification models were as follows, according to the results: 93.4% for Support Vector Machine (SVM), 93.3% for Random Forest (RF), 90.5% for K-Nearest Neighbors (KNN), and 87.9% for Decision Tree (DT). The results of the study showed that machine learning-based algorithms can produce great results for COVID-19 identification by being refined and improved using several well-known data preparation approaches.

1. INTRODUCTION

Coronavirus disease 2019, also known as COVID-19, is an infectious condition that is brought on by the severe acute respiratory syndrome coronavirus 2 (SARS-CoV-2)[1]. The first case of COVID-19 was discovered in Wuhan, China in 2019, and since then, it has quickly spread over the world, causing a pandemic that is currently affecting many different nations and areas [2]. Common COVID-19 symptoms include fever, coughing, and breathing difficulties. Additionally, some individuals may also experience loss of taste or smell, vomiting, diarrhea, sore throats, increased sputum output, and stomach pain [3]. According to information available as of April 24, 2023, the estimated death toll from COVID-19 has topped 6,860,023[4]. When someone sneezes or coughs, for example, respiratory droplets and close contact are common ways that COVID-19 spreads [5].

COVID-19 may spread by respiratory droplets, which are produced during regular breathing and through fomite transmission, which is the result of coming into touch with infected surfaces. For instance, touching the mucous membranes of the mouth, nose, or eyes after coming into contact with a contaminated surface could make it easier for the virus to enter the body [6]. This demonstrates how important it is to properly and often wash your hands. On surfaces, coronaviruses can live for several hours or even days [7]. The newly infected individual experienced symptoms on average 5.6 days after contact. Rarely, two days following exposure was all it took for symptoms to manifest. Most of those unhealthy individuals were already sick by day 14 [8]. Frequent hand washing, physical separation from others, particularly from those who are already infected, covering coughs and sneezes with tissues or inner elbows, and avoiding touching your face with unclean hands are common precautions against contracting COVID-19 [9]. The typical diagnostic technique for COVID-19 cases

*Corresponding author. Email: ghadataqa@uomosul.edu.iq

is Reverse Transcription Polymerase Chain Reaction (RRT-PCR) using a nasopharyngeal swab [10]. Moreover, a mix of risk factors and symptoms may be used to diagnose the infection [11]. X-ray pictures aid in the diagnosis of swellings, swollen lymph nodes, pneumonia, and/or lung irritation. COVID-19 examination is another application for them [12]. On the other hand, it can take some time to analyze a lot of X-ray pictures. Additionally, many healthcare providers might not have experience detecting COVID-19 because it is a novel pandemic. Creating models based on machine learning may be one way to overcome these difficulties, since they can speed up the diagnosing process and lessen the workload for medical staff at this taxing time.

2. LITERATURE REVIEWED

Using both conventional and deep learning methods, Mohammed et al. [13] presented an automatic prediction of COVID-19 identification to distinguish between healthy and COVID-19 infected people in X-ray pictures. For classification, methods like k-nearest neighbor (k-NN), decision tree (DT), radial basis function (RBF), artificial neural network (ANN), support vector machine (SVM), linear kernel, and CN 2 rule motivator were employed. Objectives. Whereas ResNet50, Google Net, Mobile Nets V2, Darknet, and Exception are located.

The collection is a sizable collection of X-ray data, with a focus on COVID-19 versus normal cases (400 healthy cases, 400 Covid cases). It is now, as far as we know, the world's largest COVID-19 dataset and has the greatest number of X-ray images of confirmed COVID-19 cases. It is feasible to draw the conclusion that all models performed satisfactorily based on the experiment findings, with the deep learning models achieving an ideal accuracy of 98.8% in the ResNet50 model. In contrast, SVM and RBF demonstrated the highest results of 95% and 94% accuracy, respectively, in classical machine learning algorithms for coronavirus disease prediction in 2019.

A pipeline for detecting COVID-19 infection using CXR images was provided by Singh et al. [14]. After extracting the features from the CXR images, the Hybrid Social Group Optimization method was used to choose the pertinent characteristics. A variety of classifiers were then employed to classify the CXR images based on the attributes that had been chosen. The suggested pipeline uses a support vector classifier to achieve 99.65% classification accuracy.

3. MATERIALS AND METHODS

Figure 3 shows the approach taken by this study to separate COVID-19 patients from other subjects using chest X-ray images. In the subsections below, each step depicted in the figure is described in detail.

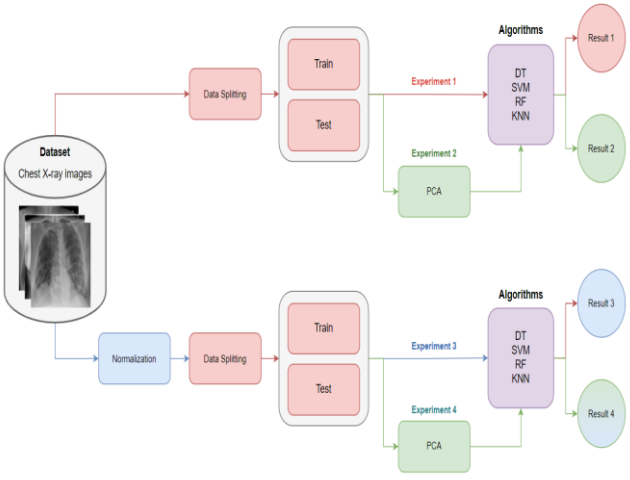

Fig.1. Schematic diagram of the proposed methodology

3.1 Dataset Collection

The COVID-19 radiography database, 2022, is accessible to the public via the Kaggle platform. Under the direction of medical specialists, a team of researchers from the Universities of Qatar in Doha, Qatar, and Dhaka University in Bangladesh created this dataset. COVID-19 and Normal chest X-ray images are included in the dataset. At the time of the investigation, there were 3,616 COVID and 10,192 Normal samples in each of the aforementioned groups.

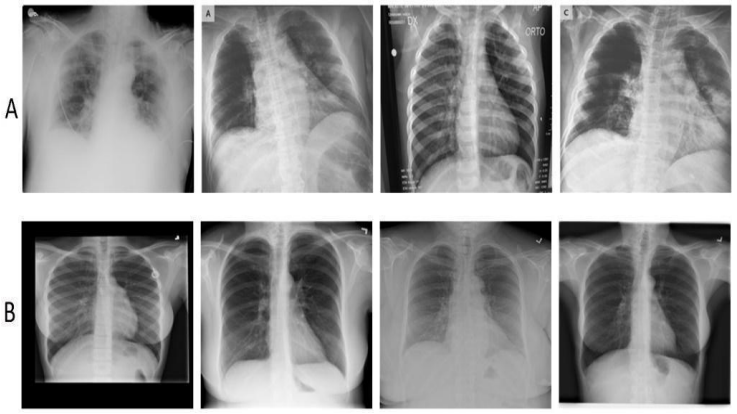

Fig .2. X-ray images were taken at different angles and locations

Figure 2 illustrates how the X-ray images were taken at different angles and locations. They were all 299 by 299 pixels in size. Because the results of this study were similar to those of other possible greater sizes, we enlarged the photos to 120 by 120. It therefore helped to speed up the training and testing procedures.

3.2 Image Normalization and Data Splitting

We conducted four trials, two of which included normalizing the picture data and the other two of which did not. By normalizing input data to have the same range and magnitude, machine learning algorithms can function more accurately and efficiently. We independently used Standard Scaling and Min-Max normalization, which are the two most often used normalization procedures. The values of min-max data range from 0 to 1. which is determined by applying the subsequent equation:

$$MinMax = \frac{X}{255} \quad (1)$$

Z-score normalization, or standard scaling, is a technique that rescales input data to have a mean of 0 and a standard deviation of 1. Standard scaling is calculated as follows:

$$Z - score = \frac{(X - X_{mean})}{X_{std}} \quad (2)$$

Every image was randomly divided into two sets, with a ratio of 80% training and 20% testing, as shown in Table I.

Table I. The number of instances used as the training and testing sets

Class Label	Training	Testing
Covid-19	***2893***	***723***
Normal	8,153	2039

3.3 PCA Overview

Principal Component Analysis, or PCA for short, is a well-liked unsupervised learning method for dimensionality reduction in machine learning. It is a statistical technique that preserves the most crucial information from the original dataset while converting high-dimensional data into a lower-dimensional space.

3.4 PCA Approach Used in Our Study

We used PCA twice in our study to achieve the objective of feature extraction. In order to improve the performance of machine learning algorithms, principal component analysis (PCA) finds a set of new variables known as principal components that are a linear combination of the original variables. We used Algorithms 1 and 2 to apply the PCA after splitting the data, as shown in table II. And III [15].

TABLE II. ALGORITHM OF FITTING PROCESS OF PCA

Input:	*Training instances:* $X^{tr} \in R^{m \times n}$
Output:	*Mean vector* (μ) *and eigenvectors* (ξ)
Step1.	*Read* X^{tr}
Step2.	*Compute the mean vector:* $\mu = \frac{1}{m}\sum_{i=1}^{m} X_i^{tr}$, *where* $\mu \in R^n$
Step3.	*Compute the covariance matrix:* $C = \frac{(X^{tr}-\mu)^T(X^{tr}-\mu)}{m-1}$, *where* $C \in R^{n \times n}$
Step4.	*Compute the eigenvalues* (λ) *and eigenvectors* (ξ) *from* C *matrix*
Step5.	*Sort the eigenvectors* $\xi_1, \xi_2, \ldots, \xi_n$ *according to their corresponding eigenvalues, such that* $\lambda_1 \geq \lambda_2 \geq \cdots \geq \lambda_n \geq 0$

TABLE III. ALGORITHM OF TRANSFORMING PROCESS OF PCA

Input:	μ, ξ, k (number of desired components), and instances to be transformed: $X \in R^{p \times n}$
Output:	Transformed instances (Z)
Step1.	Read μ, ξ, k, and X
Step2.	Select the top k eigenvectors: $F = \xi[:, :k]$
Step3.	Transform X to principal components: $Z = (X - \mu)F$, where $Z \in R^{p \times k}$

Our methodology ends with the prediction procedure, which we carried out using four classifiers that we had previously trained and fed, either with or without PCA data. These classifiers consist of KNN, SVM, DT, and RF.

3.5 Machine Learning Classification

In many fields, machine learning has become a vital tool for resolving challenging issues. Applying machine learning approaches to real-world issues has become simpler with the availability of machine learning packages like scikit-learn [16]. There are many classification algorithms that are available in the literature, in the following subsection we will mention those algorithms that are used in our study. K-*NEEREST NEIGHBOURS (K-NN*) ,Support Vector Machine (SVM),Decision tree Random Forest Classifier.

3.6 Evaluation Metrics

Numerous evaluation measures generated from the confusion matrix were employed to assess the effectiveness, advantages, and disadvantages of our suggested models. The following formula provides the metrics that are used: accuracy, sensitivity, specificity, and F1-score.

The ratio of accurately predicted samples by the model to all tested samples is known as accuracy. The percentage of accurately anticipated positive results among all actual positive samples is known as sensitivity. The fraction of accurately predicted normal samples among all actual normal samples is known as specificity. The fraction of genuine positive predictions out of all positive predictions is measured by precision, while the fraction of true positive predictions out of all actual positive instances in the data is measured by recall. The F1-Score is computed as the harmonic mean of precision and recall.

$$\boldsymbol{Accuracy} = \frac{\boldsymbol{TP + TN}}{\boldsymbol{TP + TN + FP + FN}} \times \mathbf{100}\ (\%)$$

$$\boldsymbol{Sensitivity(TruePositiveRate)} = \frac{\boldsymbol{TP}}{\boldsymbol{TP + FN}} \times \mathbf{100}(\%)$$

$$\boldsymbol{Specificity\ (True\ Negaitive\ Rate)} = \frac{\boldsymbol{TN}}{\boldsymbol{TN + FP}} \times \mathbf{100}\ (\%)$$

$$\boldsymbol{precision} = \frac{\boldsymbol{TP}}{\boldsymbol{TP + FP}} \times \mathbf{100}\ (\%)$$

$$\boldsymbol{recall} = \frac{\boldsymbol{TP}}{\boldsymbol{TP + FN}} \times \mathbf{100}\ (\%)$$

$$\boldsymbol{F1 - score} = \mathbf{2} * \frac{\boldsymbol{precision} * \boldsymbol{recall}}{\boldsymbol{precision} + \boldsymbol{recall}} \times \mathbf{100}\ (\%)$$

where the number of successfully predicted samples is represented by TP and TN. In the meantime, the number of wrongly predicted samples is represented by FP and FN.

4. RESULTS AND DISCUSSION

Python was the programming language we used to implement the suggested models on a Windows 11 machine equipped with an Intel(R) Core (TM) i5-8300H CPU running at 2.30GHz, 2304 Mhz, and 16 GB of RAM.

4.1 Hyper parameters

After conducting numerous experiments, we opted to mostly adhere to the default settings listed in Table II and not experiment too much with the hyper parameters.

TABLE IV. THE HYPER PARAMETERS USED FOR EACH CLASSIFICATION MODEL

Classification models	***Hyper Parameters***	***Parameter Values***
Decision tree	*Criterion*	*Entropy*
Random Forest	*Default*	*Ø*
K-Nearest Neighbors	*N_neighbors*	*8*
Support Vector Machine	*Default*	*Ø*

4.2 Confusion Matrix

The forecast outcomes of a certain classification method are summarized in this matrix. Its easy-to-observe confusion points in the model are the source of its name. That is, assigning a different class label to some samples. The best confusion matrix results from all four classifiers are displayed in Fig. 3. As we can see, the DT model has the highest number of misclassified samples (182 samples were misclassified as positive and 178 as negative). SVM, on the other hand, has the least incorrectly categorized samples; 115 instances were incorrectly labeled as normal, while 67 cases were incorrectly identified as COVID-19.112 instances were incorrectly classified by KNN as COVID-19, and 151 cases as Normal. Ultimately, with only 45 cases of COVID-19 misclassified, RF has performed exceptionally well.

The following math formula calculates the Error Rate for each algorithm:

$$ErrorRate = \big((FalsePositives + FalseNegatives)\big)/(TotalCases) \quad (3)$$

SVM = 6.5%, RF = 6.6%, KNN = 9.5%, and finally DT = 13.0%. The imaging similarities between COVID-19 and normal samples, along with the misalignment and non-frontal perspective of some of these samples, may have contributed to the misdiagnosis. Each image should be resized from 299 to 120 to avoid losing any features and to complicate prediction. Given SVM's low misclassification rates, it's reasonable to conclude that SVM, the suggested model, produced the best results overall.

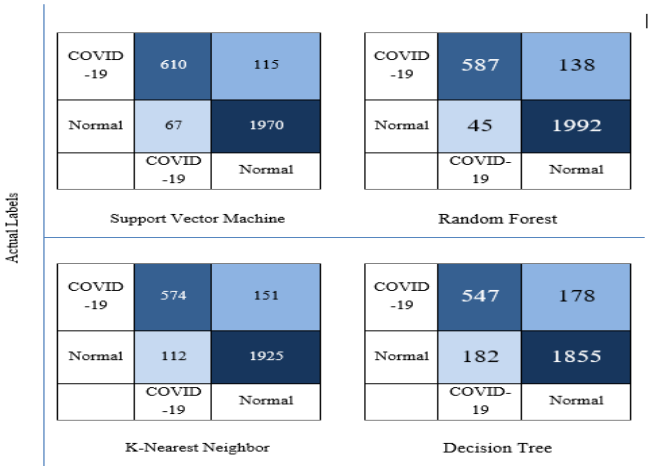

Fig .3. Confusion matrix for SVM, RF, KNN and DT

Out of all the confusion matrices, Figure 3 displays the top four outcomes. When SVM is normalized using the conventional scaler procedure and PCA is done, at least 95% of the variation in the original data may be explained by the primary components that were kept. The Min Max Algorithm was utilized to normalize DT and KNN.

TABLE V. RESULTS OF THE FOUR CLASSIFIERS USED FOR COVID-19 DETECTION UNDER FOUR DIFFERENT EXPERIMENTS

ID	Model	Type of Data	Accuracy	Sensitivity	Specificity	F1-Score
1	Support Vector Machine	Raw Data	91.6%	77.5%	96.6%	91.4%
2	Support Vector Machine	Standard Scaled Data	93.3%	83.7%	96.8%	93.3%
3	Support Vector Machine	Minmax Data	91.7%	78.1%	96.6%	91.5%
4	Support Vector Machine	Raw & PCA95	93.1%	82.3%	96.9%	93.0%
5	Support Vector Machine	Raw & PCA90	92.6%	80.7%	96.9%	92.5%
6	Support Vector Machine	Raw & PCA85	90.7%	77.1%	95.6%	90.6%
7	Support Vector Machine	Standard Scale & PCA95	93.4%	84.1%	96.7%	93.3%
8	Support Vector Machine	Standard Scale & PCA90	93.1%	83.4%	96.5%	93.0%
9	Support Vector Machine	Standard Scale & PCA85	92.4%	81.8%	96.1%	92.3%
10	Support Vector Machine	Minmax & PCA95	93.1%	82.3%	96.9%	93.0%

11	Support Vector Machine	Minmax & PCA90	92.6%	81.0%	96.7%	92.5%
12	Support Vector Machine	Minmax & PCA85	90.8%	77.0%	95.7%	90.6%
13	Random Forest	Raw Data	93.3%	80.4%	97.8%	93.1%
14	Random Forest	Standard Scaled data	93.1%	79.7%	97.8%	92.9%
15	Random Forest	Minmax Data	93.2%	79.9%	98.0%	93.1%
16	Random Forest	Raw & PCA95	83.7%	40.7%	99.1%	81.3%
17	Random Forest	Raw & PCA90	87.5%	57.7%	98.1%	86.5%
18	Random Forest	Raw & PCA85	88.0%	64.3%	96.4%	87.4%
19	Random Forest	Standard Scale & PCA95	84.1%	43.0%	98.7%	81.9%
20	Random Forest	Standard Scale & PCA90	87.8%	60.8%	97.4%	87.0%
21	Random Forest	Standard Scale & PCA85	88.5%	65.1%	96.9%	87.9%
22	Random Forest	Minmax & PCA95	84.6%	44.4%	99.0%	82.6%
23	Random Forest	Minmax & PCA90	86.8%	56.1%	97.7%	85.7%
24	Random Forest	Minmax & PCA85	87.7%	62.6%	96.6%	87.0%
25	K-Nearest Neighbors	Raw Data	90.2%	79.7%	93.9%	90.1%
26	K-Nearest Neighbors	Standard Scaled Data	90.4%	79.2%	94.4%	90.3%
27	K-Nearest Neighbors	Minmax Data	90.2%	80.4%	93.7%	90.2%
28	K-Nearest Neighbors	Raw & PCA95	90.4%	79.0%	94.4%	90.3%
29	K-Nearest Neighbors	Raw & PCA90	90.2%	77.7%	94.7%	90.1%
30	K-Nearest	Raw & PCA85	89.5%	75.9%	94.4%	89.3%

	Neighbors					
31	K-Nearest Neighbors	Standard Scale & PCA95	90.4%	77.9%	94.8%	90.3%
32	K-Nearest Neighbors	Standard Scale & PCA90	90.5%	77.8%	95.0%	90.3%
33	K-Nearest Neighbors	Standard Scale & PCA85	90.4%	77.7%	94.9%	90.2%
34	K-Nearest Neighbors	Minmax & PCA95	90.5%	79.2%	94.5%	90.4%
35	K-Nearest Neighbors	Minmax & PCA90	90.4%	77.8%	94.8%	90.2%
36	K-Nearest Neighbors	Minmax & PCA85	89.6%	76.0%	94.5%	89.5%
37	Decision Tree	Raw Data	87.5%	76.1%	91.6%	87.5%
38	Decision Tree	Standard Scaled Data	87.4%	76.0%	91.5%	87.4%
39	Decision Tree	Minmax Data	87.9%	75.9%	92.2%	87.9%
40	Decision Tree	Raw & PCA95	80.3%	62.2%	86.8%	80.3%
41	Decision Tree	Raw & PCA90	80.7%	63.9%	86.7%	80.7%
42	Decision Tree	Raw & PCA85	80.2%	65.4%	85.5%	80.4%
43	Decision Tree	Standard Scale & PCA95	80.2%	59.6%	87.5%	80.0%
44	Decision Tree	Standard Scale & PCA90	82.2%	64.3%	88.6%	82.1%
45	Decision Tree	Standard Scale & PCA85	82.9%	65.9%	88.9%	82.8%
46	Decision Tree	Minmax & PCA95	79.5%	62.9%	85.4%	79.6%
47	Decision Tree	Minmax & PCA90	79.7%	61.4%	86.2%	79.7%
48	Decision Tree	Minmax & PCA85	81.7%	64.8%	87.7%	81.7%

Despite the fact that 95% of KNN applications have utilized PCA, DT has not. Not to mention, RF achieved remarkable outcomes without the use of PCA or any normalizing methods.

4.3 Overall Performance

Figure 4 shows the route we took with our project. We ran four experiments and got 48 results in all, which are shown in Table 3. The type of data utilized to feed the categorization algorithms informed the design of these investigations.

In the first trial, we supplied digital data from picture conversion straight into the classifiers. In this experiment, the Random Forest model had the highest accuracy, coming in at 93.3%. In the second trial, we used Principal Component Analysis on the data, and the Support Vector Machine (SVM) model produced a little lower accuracy of 93.1%. Using the Standard Scale and Minmax algorithms to standardize the data for the third trial, SVM fared better than other classifiers with an accuracy of 93.3%. Ultimately, we used PCA to analyze the normalized data in the fourth experiment, and SVM produced the best results of all four with the maximum accuracy of 93.4%.

We discovered that, in terms of processing time, the RF algorithm was the quickest. Compared to other algorithms, the SVM method produced results significantly more slowly even though its accuracy was 0.1% higher. To be more precise, SVM required over an hour to finish without the use of PCA; by comparison, the Random Forest (RF) method processed data considerably faster, averaging about 8 seconds for all experiments.

4.4 Comparative Analysis with State-of-the-art Approaches

By contrasting them with other models that have been published in the literature, we assessed how well our suggested machine learning models would identify COVID-19. However, because of variations in the dataset sizes utilized in earlier research, it was difficult to compare their performance directly. When the COVID-19 outbreak was first starting, many earlier research had trouble getting enough samples, but as time went on, more samples became available via open repositories like GitHub and Kaggle. Tables 4 provide our comparison analysis's findings.

TABLE VI. COMPARE OUR MODEL TO THE EXISTING ONES

ID	Reference	Method	Data Size		Accuracy (%)
			COVID-19	Normal	
1	(Singh et al, 2021)	SVM	371	1341	99.65
2	(Mazin Abed Mohammed et al, 2020)	SVM	400	400	95.0
3	Proposed Model	SVM	3,616	10,192	93.4

It was difficult for us to locate other research that used the same methodology as ours. But we also found that SVM was acknowledged as an effective machine learning model and used in a few of that research. For this reason, in order to assess the efficacy of our study, we decided to solely compare its performance with the SVM model. When testing new samples, we doubt the validity of the results from the initial reference. It's probable that the dataset they utilized contributed to overfitting, which inflates performance outcomes.

5. CONCLUSION

The goal of scientists' and researchers' persistent efforts and ceaseless research has been to use X-ray pictures to diagnose COVID-19. They have revolutionized medical science by enabling faster and more accurate disease diagnosis thanks to state-of-the-art computer science. Deep learning models have been the standard for many studies in this field, fueled by cutting-edge technology and reliable computer systems. However, there is a research vacuum concerning the application of machine learning methods for COVID-19 diagnosis.

Driven by the paucity of study in this intriguing field, we set out on our own investigation with the goal of investigating novel algorithms and contrasting them with the ones that already existed. The outcomes were remarkable. Impressively, our (SVM) model has a 93.4% accuracy rate. We will not be satisfied to end here. With an insatiable passion for innovation, we focused on the future. Our next course of action is obvious: in order to improve our models' performance even more, we will use sophisticated image pre-processing methods. Our goal is to fully grasp the possibilities of our research and determine how well it might work in practical settings. Our vision went beyond what was possible in the lab. We imagined

our models being applied in real-world healthcare situations, positively influencing patients' lives in a noticeable way. We gladly accepted the challenge, understanding that it would open the door to more advancements and modifications. Although the road ahead is unknown, we are prepared to press on and give it our all.

Funding

No grant or sponsorship is mentioned in the paper, suggesting that the author received no financial assistance.

Conflicts Of Interest

The author’s declares no conflicts of interest with regard to the subject matter or findings of the research.

Acknowledgment

The authors would like to express their deep thanks to the college of Science, university of Zakho and the College of Dentistry, University of Mosul \ Mosul/Iraq for their provided facilities that help in this work.

References

[1] M. S. K. Mohammed, M. M. Taha, E. M. Taha, and M. N. Mohammad, "Cluster analysis of biochemical markers as predictor of COVID-19 severity," Baghdad Science Journal, vol. 19, no. 6 (Suppl.), pp. 1423-, Dec. 2022.
[2] Z. Allam, "The first 50 days of COVID-19: a detailed chronological timeline and extensive review of literature documenting the pandemic," in Surveying the Covid-19 pandemic and its implications, 2020, p. 1.
[3] CDC, "COVID-19 and Your Health," Centers for Disease Control and Prevention, Feb. 11, 2020. [Online]. Available: https://www.cdc.gov/coronavirus/2019-ncov/symptoms-testing/symptoms.html. [Accessed: Apr. 24, 2023].
[4] World Health Organization, "Getting your workplace ready for COVID-19: how COVID-19 spreads, 19 March 2020 (No. WHO/2019-nCov/workplace/2020.2)," World Health Organization, 2020.
[5] H. R. Güner, İ. Hasanoğlu, and F. Aktaş, "COVID-19: Prevention and control measures in community," Turkish Journal of Medical Sciences, vol. 50, no. 9, pp. 571-577, 2020.
[6] Z. Wang, Y. Fu, Z. Guo, J. Li, J. Li, H. Cheng, B. Lu, and Q. Sun, "Transmission and prevention of SARS-CoV-2," Biochemical Society Transactions, vol. 48, no. 5, pp. 2307-2316, Oct. 2020.
[7] National Institutes of Health and National Institute of Allergy and Infectious Diseases (NIAID), "New coronavirus stable for hours on surfaces," National Institutes of Health (NIH), 17, 2020.
[8] A. H. Ahmed, M. N. Al-Hamadani, and I. A. Satam, "Prediction of COVID-19 disease severity using machine learning techniques," Bulletin of Electrical Engineering and Informatics, vol. 11, no. 2, pp. 1069-1074, Apr. 2022.
[9] J. S. Wu, X. Font, and C. McCamley, "COVID-19 social distancing compliance mechanisms: UK evidence," Environmental Research, vol. 205, p. 112528, Apr. 2022.
[10] S. M. Alnedawe and H. K. Aljobouri, "A new model design for combating COVID-19 pandemic based on SVM and CNN approaches," Baghdad Science Journal, 2023.
[11] T. Ai, Z. Yang, H. Hou, C. Zhan, C. Chen, W. Lv, Q. Tao, Z. Sun, and L. Xia, "Correlation of chest CT and RT-PCR testing for coronavirus disease 2019 (COVID-19) in China: a report of 1014 cases," Radiology, vol. 296, no. 2, pp. E32-E40, Aug. 2020.
[12] M. T. Tsakok and F. V. Gleeson, "The chest radiograph in heart disease," Medicine, vol. 46, no. 8, pp. 453-457, Aug. 2018.
[13] M. A. Mohammed, K. H. Abdulkareem, B. Garcia-Zapirain, S. A. Mostafa, M. S. Maashi, A. S. Al-Waisy, M. A. Subhi, A. A. Mutlag, and D. N. Le, "A comprehensive investigation of machine learning feature extraction and classification methods for automated diagnosis of COVID-19 based on X-ray images," Computers, Materials & Continua, vol. 66, no. 3, Mar. 2021.
[14] A. K. Singh, A. Kumar, M. Mahmud, M. S. Kaiser, and A. Kishore, "COVID-19 infection detection from chest X-ray images using hybrid social group optimization and support vector classifier," Cognitive Computation, pp. 1-3, Mar. 2021.
[15] D. Hassan, H. I. Hussein, and M. M. Hassan, "Heart disease prediction based on pre-trained deep neural networks combined with principal component analysis," Biomedical Signal Processing and Control, vol. 79, p. 104019, Jan. 2023.
[16] M. M. Hassan and N. Amiri, "Classification of imbalanced data of diabetes disease using machine learning algorithms," Age (years), vol. 21, no. 81, pp. 33-24, 2019.